

Article

Identification of Aerodynamic Tonal Noise Sources of a Centrifugal Compressor of a Turbocharger for Large Stationary Engines

Jiří Vacula *  and Pavel Novotný 

Institute of Automotive Engineering, Faculty of Mechanical Engineering, Brno University of Technology, Technická 2896/2, 616 69 Brno, Czech Republic; novotny.pa@fme.vutbr.cz

* Correspondence: jiri.vacula@vutbr.cz

Abstract: The aerodynamics of centrifugal compressors is a topical issue, as the vibrations and noise reduce the comfort of people who are in proximity to the compressor. The current trend in rotating machinery research is therefore not only concerned with performance parameters but also increasingly with the effect on humans. An analysis of aerodynamic noise based on external acoustic field measurements may be a way to assess the nature of aerodynamic excitation. In this research, the experimental measurements at 20 operating points covered the entire characteristic operating range of the selected centrifugal compressor. The dominant noise arising at blade-passing frequency (BPF) was identified at all the operational points, and the dominant effect of the buzz-saw noise was identified at the maximum rotor speed. The determination of the total sound pressure level $L_p(A)$ showed a trend towards an increasingly higher rotor speed and compressor surge line. In the amplitude-frequency characteristics, the sound pressure was found to be dependent on the rotor speed for BPF. On the other hand, non-monotonicity was detected between the operational points at given speed lines, confirming the complexity of the aerodynamics of rotating machines. The metric chosen to identify prominent tones determined by the tonality of individual tones in the frequency spectrum showed a clear effect of integer multiples of the rotational frequency on the overall noise. Thus, the results presented here confirm the dominant influence of BPF in terms of the psychoacoustic impact on humans.

Keywords: centrifugal compressor; noise; surge; rotating stall



Citation: Vacula, J.; Novotný, P. Identification of Aerodynamic Tonal Noise Sources of a Centrifugal Compressor of a Turbocharger for Large Stationary Engines. *Appl. Sci.* **2023**, *13*, 5964. <https://doi.org/10.3390/app13105964>

Academic Editors: Alessandro P. Daga and Luigi Garibaldi

Received: 10 March 2023

Revised: 8 May 2023

Accepted: 8 May 2023

Published: 12 May 2023



Copyright: © 2023 by the authors. Licensee MDPI, Basel, Switzerland. This article is an open access article distributed under the terms and conditions of the Creative Commons Attribution (CC BY) license (<https://creativecommons.org/licenses/by/4.0/>).

1. Introduction

Centrifugal compressors are used for turbocharged gas or diesel engines of ships and for engines used in heat and power generation. More engine power is often associated with higher compressor pressure ratios and therefore higher rotor speeds, which then cause secondary problems due to increased noise levels. In recent decades, there has been significant progress in the understanding of and reduction in different types of turbocharger noise. For radial centrifugal compressors, the achievements do not appear to be as significant. This may be partly due to their specific geometry incorporating different control strategies to extend the range of the operating conditions. This makes it difficult to perform complex numerical studies or acoustic optimisation procedures, as the time required to run these simulations quickly becomes excessive. In addition, in the past, radial compressors were often installed in applications where weight was not of significant importance and where isolation was possible. However, the regulatory framework for acoustic emissions is changing, and low noise levels may become another selling point in many applications.

Of particular importance is the tendency of turbochargers to increase the operating speed, which has a significant impact on the overall noise level of the compressor. The acoustic performance of the compressor increases by an order of magnitude of 5 and higher

powers of compressor speed. It is worth noting that the high speed of a rotary machine and related noise is nowadays not only an issue in the field of radial compressors but also in other transport-related equipment. Thus, external acoustic field experimental testing is widely used to detect and assess the possible sound sources [1,2]. Compressor noise typically contains many different noise sources, with the dominant noise source under virtually all operating conditions being rotary tonal sound.

Noise and vibration in centrifugal compressors has been a research subject for decades. The first experimental projects that focused on analysing rotating stall and its detection were studies by Jansen [3] and Lennemann and Howard [4]. Their research on rotating flow instabilities was followed by studies that focused on furthering the knowledge and on rotating flow instability suppression. Such studies were carried out by Senoo and Kinoshita [5,6] and Senoo and Ishida [7], who researched tip clearance losses. In addition, broad research into compressor surge was conducted by Greitzer [8,9]. Their research, although carried out in the field of axial compressors, laid the theoretical foundation for centrifugal compressors. The development of axial machines used to be a step ahead of that of radial machines, mainly because of their wider application and higher efficiency. This was reflected in the research on sound generated aerodynamically [10] and in studies on, for example, casing treatments aiming to influence efficiency or aerodynamic sound [11–13]. However, as automotive turbocharging became more widespread, research on centrifugal compressors' stable operation and aerodynamic noise generation increased [14–16].

The ability to correctly predict blade-passing frequency (BPF) noise has become the subject of not only experimental research but also the development of numerical and analytical procedures. As shown by, for example, Sun and Lee [17], Ohta et al. [18] and Ingenito and Roger [19], rotational noise is the main source of noise in centrifugal compressor operation. In the last few years, research on centrifugal compressor tonal noise has begun to move in the direction of modelling using computational fluid dynamics (CFD) [20–22], and the reduction in noise has even become an objective function in the automatic optimisation of aerodynamic design, as shown by Wan et al. [23]. Experimental testing confirming BPF to be the dominant sound source in centrifugal compressors can be found in the work by Mao et al. [24].

BPF is a typical problem with centrifugal compressors and can have a variety of causes. This type of noise is usually characterised by a high-pitched whining sound that is caused by the impeller passage passing over the tongue. Rotary tonal noise can be annoying and can interfere with the normal operation of the equipment. In addition, it can be a sign of hidden problems that can affect the performance and reliability of the compressor. Particularly at high blade tip speeds, when gas velocities locally reach supersonic speeds, a second typical noise of centrifugal compressors occurs. This noise, known as buzz-saw noise, is due to the shock waves in the compressor.

Noise containing tonal frequency components is particularly unpleasant for humans from a psychoacoustic point of view. Tonality, as a psychoacoustic indicator, identifies the emerging tones above the background noise and determines their contribution to the perception of sound. The tonality of an acoustic source is one of the main metrics generally monitored to improve the sound quality of a product, along with the loudness, steepness, harshness and the strength of the fluctuations. Quantifying tonality means translating how tonal sound is perceived by the human ear as objective metrics. In industrial applications such as automotive, aviation, rail or consumer goods, tonality expresses the relative weight of the tonal components over their ambient frequency content. Tonality in rotary machines has become a research topic in terms of the psychoacoustic impact on humans in different fields, ranging from the aviation industry [25] to household equipment, such as vacuum cleaners [26].

Generally, the most effective way to achieve quieter machines is through a design change affecting a specific component or interaction of components. However, any changes require identifying the specific source of the noise at the compressor. Identification based on the sound of an existing compressor requires considering not only the measured sound

in the form of pressure time history itself but also the operating condition of the centrifugal compressor and comparing these with the existing knowledge of clearly defined noise sources. A detailed description of the aerodynamic processes in the compressor requires rather demanding CFD simulations, as summarised in, for example, the work by Vacula and Novotný [27], and in most cases are unavailable. A general overview of the noise sources in centrifugal compressors can be found in, for example, [28,29].

The aerodynamic noise sources in the centrifugal compressor are particularly dominant at higher speeds and can mask mechanical noise to a large extent. Mechanical noise, usually caused by the rotation of the unbalanced mass or even instabilities in the lubrication layer of the hydrodynamic bearings, can be identified in frequency domains but has little effect on the overall sound power level. The aim of this experimental study was to find and analyse the tonal types of noise in high-speed and high-pressure centrifugal compressors and to analyse the operating conditions leading to the tonal types of noise based on the parameters defining the centrifugal compressor operation. Many observations can be found in the literature [28,30–32], where authors indicated the possibility of certain characteristic types of noise, such as tip clearance noise (TCN), noise due to rotating stall and broadband noise, occurring under off-design conditions. The aim of this paper is to show, by means of a specific case study, what types of noise were produced by the compressor presented here during operation and which can be considered the most audible to the human ear.

2. Typical Aerodynamic Noise Characteristics of High-Speed High-Pressure Centrifugal Compressors

Aerodynamic and mechanical phenomena occurring in centrifugal compressors can be characterised by their excitation frequency f . This excitation frequency can then be identified in terms of the vibration, sound pressure, axial forces, stresses and similar factors. The rotational frequency f_R of the rotor is a fundamental parameter of a rotating machine and can be used to describe the vibroacoustic characteristics with relation to aerodynamic processes. Thus, the excitation frequency can be related to the rotor speed, and the excitation frequency ratio of a given phenomenon can be defined as

$$\varepsilon_R = \frac{f}{f_R}. \quad (1)$$

The excitation frequency ratio requires knowledge of the instantaneous rotor speed, but this parameter is normally determined in engineering experiments. Thus, in practice, it can conveniently replace frequency in tonal source identification methods. The ability to identify certain types of noise requires reliable knowledge of the frequency characteristics of these types of noise. The advanced global literature contains a large amount of information that can be evaluated, and a metric for identifying tonal noise types can be established with sufficient reliability.

2.1. Rotating Blade-Related Noise

An important source of the excitation in turbomachinery is the interaction between the rotating blades and the stationary parts, known as rotor-stator interaction (RSI). The corresponding excitation is due to the interaction of the flow field with the stator parts of the turbomachine. The excitation frequency is then typically an integer multiple κ of the rotor speed f_R , and the resulting frequency of super-harmonic noise is defined by the equation

$$f = \kappa f_R. \quad (2)$$

As a result of the interaction between the rotor and the stator, the flow field may be disturbed, and this disturbance may be gradually transmitted through the individual blade-to-blade passages in the form of a rotating stall. Essentially, this is an unsteady flow field that interacts with the turbomachine, causing vibration and noise in the rotating machine. These rotating cells usually rotate at a lower speed than the rotational speed of

the impeller. The equation describing the possible number of super-harmonic multiples arising in possible aerodynamic modes due to RSI can be written as

$$\kappa = \kappa_R z_R \pm \kappa_S z_S, \quad (3)$$

where κ represents the number of stall cells of the rotating stall, and κ_R and κ_S are harmonic multiples of the number of rotor blades z_R and stator vanes z_S , respectively. In the frequency spectrum, this type of noise occurs particularly at high rotor speeds and can be identified as a tonal type of sound. This sound is very distinct for most centrifugal compressors. A typical representative is rotary tonal noise due to the interaction of individual blades and the tongue of the volute housing (rotating blade-related noise). In terms of frequency, this tonal noise occurs at integer multiples of the rotational frequency, and the corresponding frequency ratio of the tonal components of rotating blade-related noise can be defined as

$$\varepsilon_{R,RBR} = \kappa. \quad (4)$$

Typical examples of centrifugal compressor rotational noise occurring at BPF were presented by Chen [33]. In addition, Raitor and Niese [28] described the effect of the generated tonal sound in the centrifugal compressor piping, with the amplitudes of this tonal sound in the outlet duct being higher than in the inlet duct. This clearly shows that the RSI is the dominant factor in the generation of sound in the outlet pipe. Other examples of rotational tonal noise can be found in [20,34,35].

2.2. Buzz-Saw Tonal Noise

If a centrifugal compressor is operated under conditions where the relative velocity at the leading edges of the impeller blades approaches the local speed of sound, shock pressure waves are generated in the passage between the impeller blades [36]. The main cause of buzz-saw noise is the rotor's pressure field, which is stable in the rotating (relative) coordinate system, that is, the pressure field coupled with the rotor. In the case of a completely ideal rotor operating in a uniform flow field, the individual shock waves generated by all blades are the same. In such a case, the shock waves can be simplified in the form of repeating the one-dimensional sawtooth waves. An analytical description of this idealised case can be found in the research by Morfey and Fisher [37]. Their work was followed by that of many other authors, who gradually expanded the description of buzz-saw type noise. A summary of the development of methods describing this type of noise can be found in a study by Tang and Li [38], for example. However, in real rotating machines, individual blades exhibit minor geometric variations. These deviations result in different amplitudes and different shifts between the individual shocks and therefore affect their propagation, which is nonlinear. Thus, these small irregularities ultimately lead to spectral components present at integer multiples of the rotational frequency. The frequency ratio of the individual tonal components of the buzz-saw noise can be defined as

$$\varepsilon_{R,BS} = i, \quad (5)$$

where $i = 1, 2, 3 \dots$ is the order of the harmonic component.

The resulting acoustic character can be observed in the form of tonal sounds at integer multiples of the rotational frequency; thus, it is a super-harmonic type of noise. These conclusions were also stated by Sharma et al. [39], Raitor and Neise [28] and Thisse et al. [40]. The description of buzz-saw noise is still a current research topic, as this type of noise is dominant in aircraft engines. In the field of aeronautics, research on the description of this noise is especially important because it is present during take-off and climb, as that is when the rotating machine is in its transonic regime. Raitor and Neise [28] stated that the dominant source of noise at the inlet of the compressor at 'high' rotor speeds is buzz-saw noise, in addition to rotational frequency and BPF. It should also be noted that there is no well-defined boundary, for example, in terms of rotor speed, that would determine the

occurrence of buzz-saw noise. For example, Raitor and Neise [28] only stated that this noise occurs at ‘supersonic tip speeds’. However, the occurrence of shock waves is caused by the exceedance of the sound speed of the flowing gas, which is local and depends to some extent on the geometry of the impeller channel. For this reason, buzz-saw noise does not occur suddenly. On the contrary, a gradual increase in the individual tonal components with an increasing compressor speed can be expected.

Additionally, Raitor and Neise [28] stated that when supersonic flow conditions occur at the inlet of a centrifugal compressor, that is, $Ma_1 > 1$, buzz-saw noise and BPF are dominant, and RSI may be present at the outlet, whereas in the case of subsonic flow conditions, that is, $Ma_1 < 0.95$, the noise associated with the interaction of the blade tip and the shroud, also known as the TCN, is evident.

2.3. Unbalance Whistle

Unbalance whistle is caused by unbalanced rotors. In general, rotor unbalance is an inherent issue to a greater or lesser degree in all rotating machines. The unbalance may even change during the operation of the rotating machine. The excitation frequency occurs at the rotational frequency. In cases where the main axis of inertia of the rotor does not lie in the axis of rotation, higher multiples of the rotational frequency may appear in the frequency spectrum. This only occurs in the case of a bent rotor or when the rotor assembly becomes loose.

The frequency ratios corresponding to the unbalance whistle introduce some inaccuracy into the identification of aerodynamic noise, since the corresponding frequencies occur at the same frequencies as the buzz-saw noise. For this reason, it is then necessary to carefully consider typical frequencies of orders one and two.

2.4. Tip Clearance Noise

As stated above, if supersonic conditions do not occur at the design point of the compressor, the significant sound may be due to flow through the tip clearance, referred to as TCN. TCN is often evident in both the inlet and outlet of the compressor. TCN frequency was found by Raitor and Niese [28] to be in the range of $f = \varepsilon_{R,TCN} f_R$, where typical values of the excitation frequency ratio are in the range of $\varepsilon_{R,TCN} = (0.36 - 0.64) z_R$. However, as reported by Raitor and Niese [28], the value of $\varepsilon_{R,TCN}$ varies with the rotor speed.

2.5. Noise of Aerodynamic Instabilities

The ability to detect the presence of aerodynamic instabilities in the operation of a centrifugal compressor is important because their presence can pose a significant risk to its safe operation. The terms ‘surge’ and ‘stall’ are encountered in the literature, and the difference between them should be noted. Under certain flow conditions, the flow may separate from the blade. This flow separation may be gradually transmitted across the individual blade-to-blade passage, which is when the rotating stall phenomenon occurs. Thus, rotating stall refers to the occurrence of rotating pressure fields that have varying numbers of maxima and minima, which may even vary in time. Essentially, this is an unsteady flow field that interacts with the turbomachine and thus causes an excitation. These pressure fields usually rotate at a lower speed than the rotational speed of the impeller; therefore, the individual blade-to-blade channels are affected. In general, stall can occur at any operating point on the compressor map, but it most often occurs at off-design operating points, that is, at very high or very low flow rates.

On the other hand, surge, as stated by, for example, Marshall and Sorokes [29], is an operating condition in which the flow in the compressor is fully recirculated, resulting in significant flow pulsations. Stall occurring in either the impeller or the diffuser can be seen as a trigger mechanism for surge or as a precursor of surge [41–43]. Some authors, such as Ribi and Gyarmathy [44], attributed the occurrence of deep surge to impeller rotating stall, that is, rotating stall due to impeller geometry. In fact, the surge line, they determined, was independent of the diffuser geometry and changed when the impeller

changed. Furthermore, Hong et al. [45] observed the dependence of the surge line on the magnitude of the tip clearance, which in principle suggests some relation between the secondary flow in the tip clearance and an initiation of surge. The presence of an emerging separation that can lead to the initiation of surge can manifest itself in increased noise, although compressor operation is not necessarily at an operational point close to the surge [46]. This is why, for example, Kämmer and Rautenberg [47] distinguished between a ‘surge line’ and a ‘stall limit line’ in the compressor map.

2.6. Aerodynamic Noise Due to Kelvin–Helmholtz Instability

It is worth mentioning Kelvin–Helmholtz instability, which, unlike rotating stall, is even more local in nature, as there is no influence across the individual blade-to-blade channels. If this instability arises, it rotates in each channel essentially the same way and can therefore be viewed as periodic. A very illustrative description of this phenomenon was offered by Bousquet et al. [48]. It involves the formation of a shear layer at the interface between the main jet and a region of low momentum close to the shroud, which leads to the non-stationary nature of the flow field in this region and, hence, to the vortex-shedding phenomenon. In the case of Kelvin–Helmholtz instability, it should be pointed out that because it is an instability essentially rotating with the impeller, its identification in a stationary coordinate system may be suppressed by the BPF, which may overlap it in the amplitude-frequency characteristics [48]. However, assuming the use of pressure probes (or monitoring points in the case of CFD analysis) distributed circumferentially in each channel of the impeller, the presence of Kelvin–Helmholtz instability can be identified. First, the time signals of the individual probes have to be phase-shifted by their pitch angle and then averaged to obtain a pressure time history representing the pressure fluctuations of all blade-to-blade passages. It should be noted that, in the absence of any local instability, the amplitudes of the signals in each channel should be nearly identical. This average value is then subtracted from the individual signals, and a Fourier transform is applied. However, as Bousquet et al. [48] pointed out, this method can be used even when using probes in a stationary system. The detection of Kelvin–Helmholtz instability can be one way to identify the stability limit, as this instability can be a precursor to rotating stall.

2.7. Surge

For surge, and especially for deep surge, it is typical that the excitation frequency ratio takes very low values, such as, for example, $\varepsilon_R < 0.04$ [16,30,43,49–51]. Therefore, it is appropriate to analyse surge phenomena in the time domain in lieu of the frequency domain. The acoustic characteristics of surge, especially in the automotive industry, may be referred to as ‘whoosh noise’ [14,31,52,53]. However, in the case of whoosh noise, also called ‘surge noise’ [34], it is not a situation where the fluid is recirculated throughout the whole compressor—that is, deep surge—but it is a rotating stall. Evans and Ward [27] used the term ‘marginal surge region’.

In addition, the surge line can be influenced by the compressor design modifications, such as the use of internal recirculation channels, the use of variable inlet guide vanes and the modification of the diffuser flow path [54]. Chen [33] pointed out the possibility of the design modifications affecting the aerodynamic noise. These impacts include the effect of the ellipticity of the trailing edge of the impeller blades on aerodynamic noise and the effect of the modification of the ported shroud type on the possibility of an increase in the BPF noise due to the presence of fins in the ported shroud. Sharma et al. [39] confirmed the negligible effect of ported shroud type modification on tonal noise. Off-design aerodynamic phenomena occurring in a centrifugal compressor remains an area of research, which is currently moving in the direction of numerical modelling using CFD tools. However, as summarised by Vacula and Novotný [27], CFD analyses of low-frequency phenomena in rotating machines require much time and hardware, as it is necessary to analyse the rotor speed with adequate time discretisation and a sufficient number of revolutions to affect the low-frequency agency simultaneously. In addition,

it is necessary to use turbulence models; thus, these are most often unsteady Reynolds-averaged Navier–Stokes equations [31,53,55,56], a detached-eddy simulation [53,56,57] or a large-eddy simulation [43,58–60].

Noise generated aerodynamically during the operation of a centrifugal compressor is one of the possible indicators of flow instabilities and machine operating quality. It can therefore be assumed that measuring the external acoustic field in the vicinity of the compressor can reveal the significant sources of the aerodynamic excitation causing not only negative noise but also undesirable vibrations.

3. Methods Used for Identification of Tonal Noise Sources

3.1. Tonal Metrics

The existence of tonality refers to the presence of a single dominant frequency or pitch in a sound. This dominant tone is usually caused by a single, constant source of vibration, such as a rotating machine that contains a single frequency component due to unbalance. Thus, when the sound produced by this vibration is analysed, a relatively strong and clearly defined tone is apparent. Tonality can be a useful indicator of certain types of problems in mechanical systems. In a centrifugal compressor, for example, tonality in the noise or vibration spectrum may indicate the presence of an unbalanced blade or entire rotor. Similarly, the tonality of the sound generated by a bearing may indicate the presence of a major malfunction.

Understanding the tonality of sound can be helpful in diagnosing problems and developing strategies to mitigate or eliminate unwanted noise and vibration. Tonal sound is perceived by humans as unpleasant. Tonality is a psychoacoustic indicator that identifies emerging tones above ambient background noise and determines their contribution to the perception of sound. The more energy there is around a frequency, the less perceptible that frequency is, and, thus, the less tonal that sound is. The presence of tonal sound is therefore significant.

In practice, when measuring compressor sound, there are constant small fluctuations in the measured quantities, even under steady-state conditions. For example, compressor speed can fluctuate by tens of revolutions per minute. Thus, periodic averaging must be used for identification. This averaging uses the knowledge of the actual rotor speed according to the speed mark. The idea is to select a short period of time when the speed variation is insignificant and to analyse this period separately. After N time periods, the entire measured signal is processed. The sound pressure amplitude of the N time steps is then determined as follows:

$$p(f) = \mathcal{F}(p(t)), \quad (6)$$

where $p(t)$ is the measured sound pressure, t is the time defined at discrete points $t = t_j \dots t_j + \Delta T$ corresponding to the sampling frequency, ΔT is a short time interval typically lasting several hundred rotor revolutions and \mathcal{F} is the discrete Fourier transform operator converting the time signal into the frequency domain. According to Equation (6), the amplitude of the sound pressure in the frequency domain is determined as a function of frequency for each time sub-interval.

In practical cases, when a compressor is measured for a long period under steady-state operating conditions, there are constant small fluctuations in the rotor speed and, therefore, in the acoustic parameters. Thus, the analysed frequency component associated with a particular aerodynamic phenomenon occurring in the compressor might continuously vary slightly within the time frame. For this reason, the amplitude-frequency characteristic $p(f)$ is converted into a dependence of the pressure amplitude on the frequency ratio $p(\varepsilon_R)$. However, due to the variability in speed, the frequency ratio must be slightly corrected according to the actual known speed f_R .

It is worth noting that in rotordynamics there is a group of well-established algorithms called order tracking which allow the measured signal to be transformed from the time domain to the angular domain with respect to the actual shaft speed. These include computed order tracking, Vold-Kalman filters and order tracking transforms. The use of

order tracking algorithms is certainly possible, but given the objective of this study, which is mainly to detect dominant tones whose level may be affected to some extent by the impedance of the environment, the procedure used here is fully justified. The tonal metrics for identifying the tonal components of noise include an algorithm that can search for tones in the frequency spectrum of the measured sound pressure. Rather than using the absolute value of the tone, the metric focuses on the position of the tone relative to the rotor speed and the tone level relative to the background sound pressure level. The distance of the tone level from the background can be defined using the tone-to-noise ratio criterion:

$$L_{\text{TNR}} = 20 \cdot \log \left(\frac{p_{\text{ef},\varepsilon_{\text{R}}}}{p_{\text{ef,noise}}} \right), \quad (7)$$

where $p_{\text{ef},\varepsilon_{\text{R}}}$ is effective pressure of the analysed excitation frequency ratio and $p_{\text{ef,noise}}$ is the effective pressure of the surrounding frequency band (masking noise) corresponding to the frequency ratio width $\varepsilon_{\text{R,band}} = 0.2$, both without the application of weighting filters.

Frequency bandwidth is quite an important parameter for the evaluation of masking noise. In cases where tonal components are sought to quantify the ability of the human ear to discriminate between different frequency tones, critical bands are used [61]. For a positive identification of a given tone from the ambient sound by a human, a minimum tone separation of 8 dB is assumed (Fastl and Zwicker [61]). However, the metric used for this research focuses on the identification of noise sources; thus, a fixed frequency bandwidth is used because critical bands are significantly wide at higher frequencies. The size of the width is chosen to allow the identification of even tones with lower amplitude. As the bandwidth increases, the identification capability is partially reduced because the lower amplitude tones are masked by the surrounding stronger tones.

Based on the tone-to-noise ratio values, the prominent tones L_{PT} are selected from the entire frequency spectrum as

$$L_{\text{PT}} = \zeta \cdot L_{\text{p}}, \quad (8)$$

where $L_{\text{p}} = 20 \cdot \log \left(\frac{p_{\text{ef}}}{p_{\text{ref}}} \right)$ is the sound pressure level from the measured effective pressure, p_{ef} , $p_{\text{ref}} = 2 \cdot 10^{-5}$ Pa is the reference sound pressure and ζ is the binary selection function.

$$\zeta = \begin{cases} 1 & \text{if } L_{\text{TNR}} \geq L_{\text{lim}} \\ 0 & \text{if } L_{\text{TNR}} < L_{\text{lim}} \end{cases} \quad (9)$$

where L_{lim} is the limiting value of the tone-to-noise ratio to select prominent tones. In the case of this study, a value of 8 dB was chosen.

After evaluating the prominent tones from the time interval, it is necessary to average the partial prominent tones from each time interval $L_{\text{PT},i}$. During this averaging, it is necessary to ensure that the frequency ratios of the individual tones are corrected according to the actual rotor speed. The average prominent tone is determined as

$$\bar{L}_{\text{PT}} = \sum_{i=1}^N L_{\text{PT},i} \quad (10)$$

The algorithm for evaluating the tonal metrics is shown in Figure 1.

In this research, the tonal metrics were applied to a set of sound pressure measurements of the centrifugal compressor of a turbocharger. Examples of partial displays of the measured signal are presented in Figure 2.

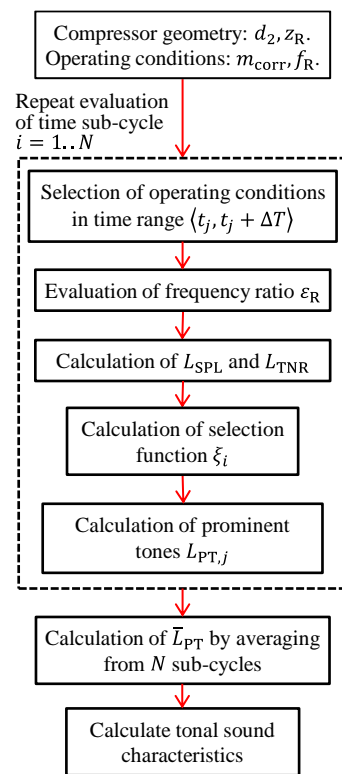


Figure 1. Schematic overview of the algorithm for evaluating tonal metrics of measured sound pressure.

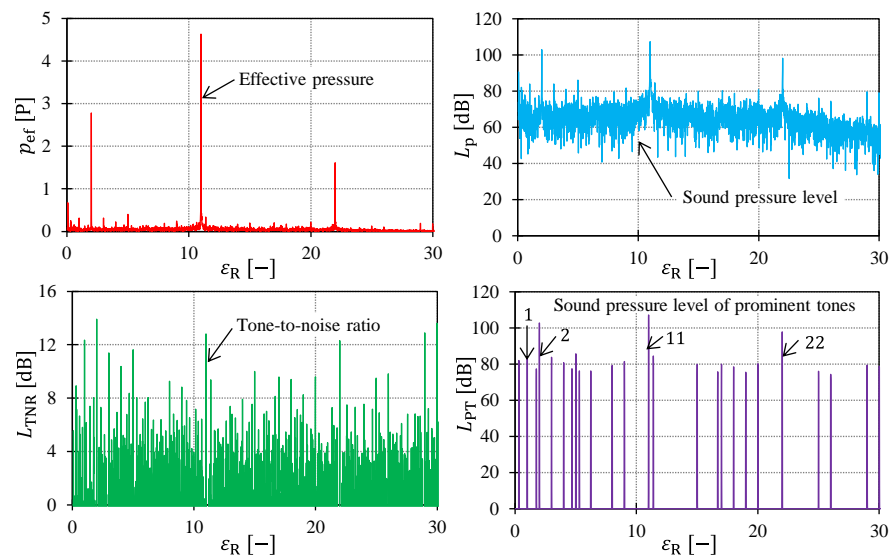


Figure 2. Partial displays of the measured signal at each step of the tonal metric evaluated from a time sub-cycle length of 0.29 s for the operating conditions of a compressor with 11 impeller blades and a vaned diffuser; corresponding blade tip speed $u_2 = 500 \text{ m}\cdot\text{s}^{-1}$.

3.2. Experimental Setup

The test facility consisted of an open-loop centrifugal compressor test rig placed in a laboratory room used for compressor performance measurement. The compressor’s surroundings thus represented a diffuse field that could have a certain influence on the amplitudes of the acoustic signal. Generally, the acoustic impedance of the test environment has a limited effect on the broadband noise, but it has a considerable effect on the tonal noise. The frequency of the signal, however, is affected negligibly. Moreover, these machines

are always placed in non-anechoic chambers when they operate. Thus, this experiment reflected the typical placing and operation of a centrifugal compressor.

The compressor drew in the ambient air at atmospheric pressure and contained an 11-bladed unshrouded impeller with a diameter of 0.231 m, a 19-vaned diffuser and a volute. At the outlet of the volute there was a 0.14 m internal diameter pipe 0.8 m in length, followed by a 0.218 m outlet diameter cone, which was followed by a 0.2 m diameter pipe with bellows, elbows and an orifice with a total length of 23 m. Total pressure and temperature sensors were placed at the inlet and outlet of the compressor. In addition, sound recording microphones were placed approximately 1 m away (Figure 3). In this way, the compressor map was measured, and the sound pressure at each operating point was measured by the microphones. During measuring, basic turbocharger operating parameters such as rotor speed, gas pressures and temperatures upstream and downstream of the compressor and turbine, oil temperature and pressure at the turbocharger inlet were also recorded.

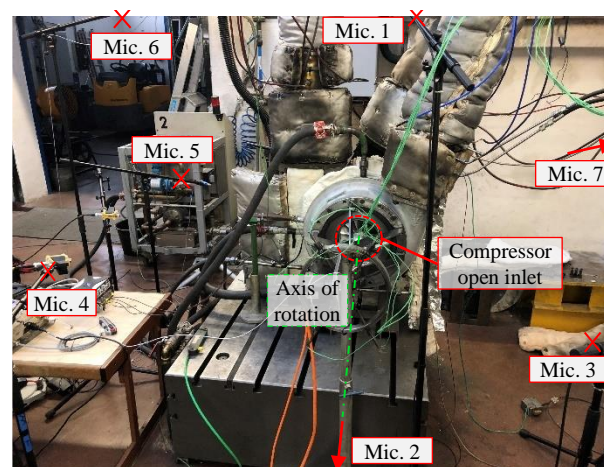


Figure 3. Setting up a set of microphones near the turbocharger compressor to be measured.

Each operating point of the compressor map was measured separately in a cycle including the run-up to the operating point, a turbocharger steady state of 10 min and the steady-state measurement of operating variables. The measurement time of the operating variables at the steady-state operating point was 22 s at a sampling rate of 65,536 Hz. Five speed lines $u_2 = 250, 350, 450, 500$ and $550 \text{ m}\cdot\text{s}^{-1}$ were measured at four operating points on each speed line (Figure 4). These points were aerodynamically approximately affine; thus, so-called ‘sweeps’ could be introduced, where the relations $m_{\text{corr}} = f(u_2)$ and $\pi_{t-t} = f(u_2^2)$ were valid. This approximate dependence held between speeds of 450–550 $\text{m}\cdot\text{s}^{-1}$ with a deviation of less than 15%. Basic information on the sensors used for the experiment is given in Table 1.

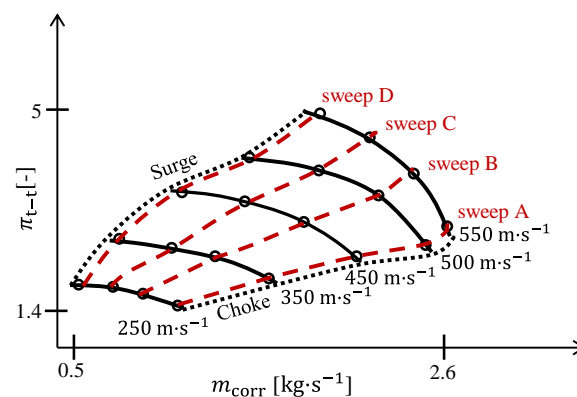


Figure 4. An illustrative overview of measured operating points expressed in the compressor map.

Table 1. List of sensor characteristics used for technical experiments.

Quantity	Sensor Type	Measurement Range	Measurement Accuracy
Sound pressure	Condenser microphone	3.1–40,000 Hz	Dynamic range: 6.5 dB to 192 dB, sensitivity 12.5 mV/Pa
Gas temperature	Thermocouple	−40–1200 °C	±1.5 °C for 0–333 °C or ± 0.75 °C for 333–1200 °C, class 1, DIN EN 60584
Gas pressure	Piezoresistive	0–1500 bar	±1% of FSO at room temperature
Oil temperature	Thermocouple	0–200 °C	±1.5 °C, class 1, DIN EN 60,584
Oil pressure	Piezoresistive	0.5–6 bar	±0.5%

4. Results and Discussion

The presence of tonal sound in the external acoustic field generated by the operation of a radial compressor can be demonstrated by plotting the amplitude-frequency characteristics of the sound pressure level in the audible spectrum. Figures 5–8 present the results of this research. These plots clearly show the presence of tonal noise, which arose at all speed lines. The amplitude-frequency characteristics were determined based on the entire duration. However, due to the slight rotor speed variations within a time frame, any aerodynamic phenomenon in the frequency domain can be represented by several frequency components. The amplitudes of these components are, however, smaller than the corresponding amplitude of the tonal component of the phenomenon at constant rotor speed. This is not apparent at any given level in Figures 5–8.

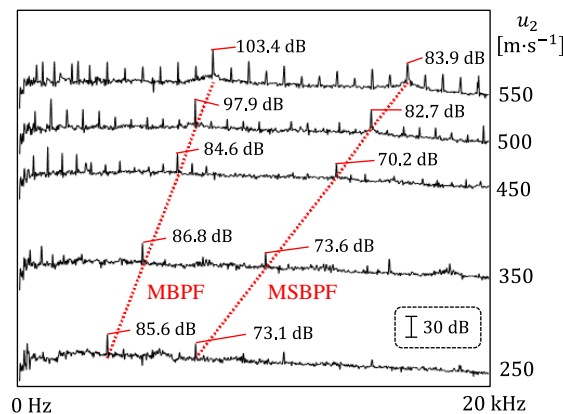


Figure 5. Sound pressure level $L_P(A)$ vs. frequency in the range 0–20 kHz, sweep A.

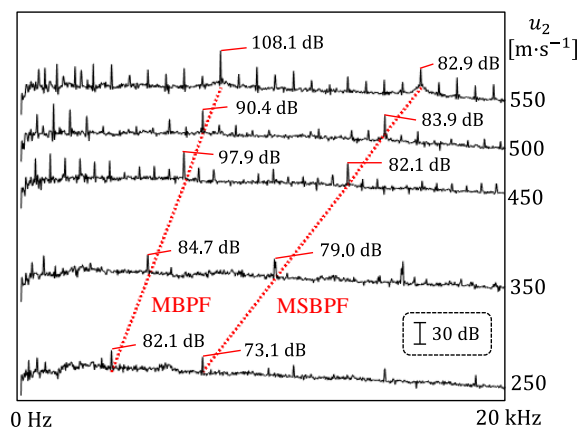


Figure 6. Sound pressure level $L_P(A)$ vs. frequency in the range 0–20 kHz, sweep B.

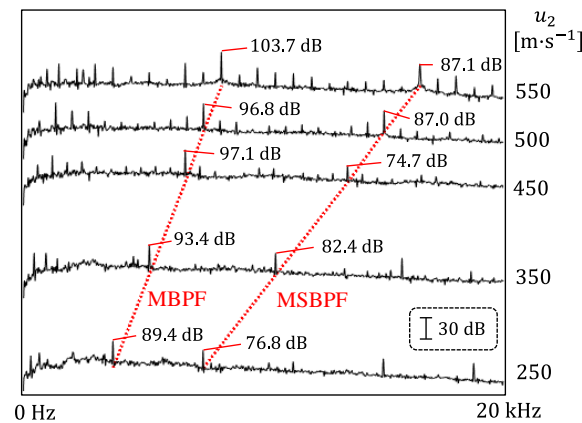


Figure 7. Sound pressure level $L_p(A)$ vs. frequency in the range 0–20 kHz, sweep C.

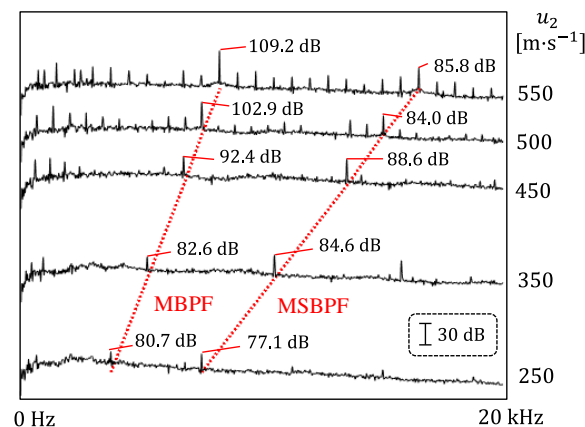


Figure 8. Sound pressure level $L_p(A)$ vs. frequency in the range 0–20 kHz, sweep D.

At all analysed speeds, rotating-blade related noise was dominant. This typically dominant noise for compressors was evident in both the blade frequency of the main blades (MBPF) and the blade frequency of the sum of the main blades and splitter blades (MSBPF). However, as the speed increased, the effect of single-integer multiples of the rotational frequency, that is, buzz-saw noise, became more evident. The buzz-saw noise was evident at higher rotor speeds $u_2 = 550 \text{ m}\cdot\text{s}^{-1}$ and $u_2 = 500 \text{ m}\cdot\text{s}^{-1}$ for all operating points (sweeps A–D). Conversely, this noise could not be uniquely identified at rotor speeds $u_2 = 250 \text{ m}\cdot\text{s}^{-1}$ and $u_2 = 350 \text{ m}\cdot\text{s}^{-1}$, which was due to the absence of supersonic aerodynamic conditions in the impeller at this rotor speed. The rotor speed $u_2 = 450 \text{ m}\cdot\text{s}^{-1}$ showed initial indications of buzz-saw noise development, with the most obvious being observed at sweep B, depicted in Figure 6.

In all sweeps (Figures 5–8), at maximum rotor speed $u_2 = 550 \text{ m}\cdot\text{s}^{-1}$, significant tonality was seen at low frequencies, but these were not integer multiples of the rotational frequency. It can also be noted that the BPF was significant at all measured points, and a distinction can be made between MBPF and MSBPF. The cause of the opposite trend with respect to all other operating points can probably be found in the rotating stall at operational points leftward from the maximum efficiency point in the compressor map at the given speed line. As for TCN, it can be seen from the depicted amplitude–frequency characteristics that there was no distinct broadband noise whose origin could be attributed to TCN in the range $\varepsilon_R = (0.36\text{--}0.64)z_R$ [27].

By evaluating the sound pressure level for the entire audible spectrum at the measured operating points of the compressor, a compressor map can be obtained that presents the total sound pressure level (Figure 9). The results presented in Figure 9 clearly show the strong expected increase in sound pressure level with compressor speed. Figure 9 therefore presents the typical characteristics of aerodynamic noise distribution in a compressor map.

However, an accurate determination of the sound pressure level would require the test setup to be placed in an anechoic chamber.

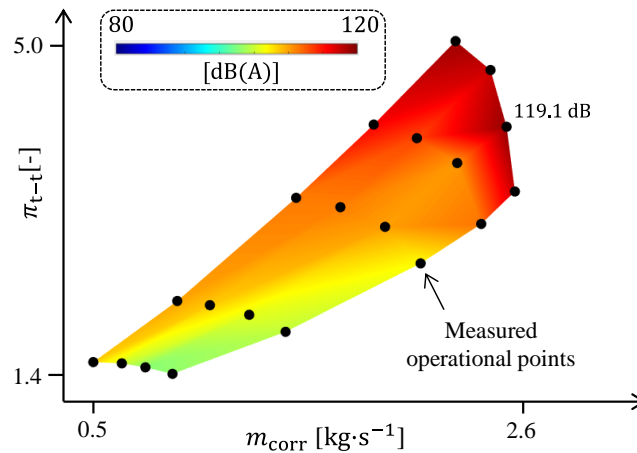


Figure 9. Compressor map showing sound pressure levels in the range of 0–20 kHz.

The presence of tonal noise was already evident in the amplitude-frequency characteristics. However, the tonal metrics were used to qualitatively evaluate the presence of tonal noises. The results of applying the tonal metrics in the form of sound pressure levels of prominent tones at sweeps A–D are presented in Figures 10–13.

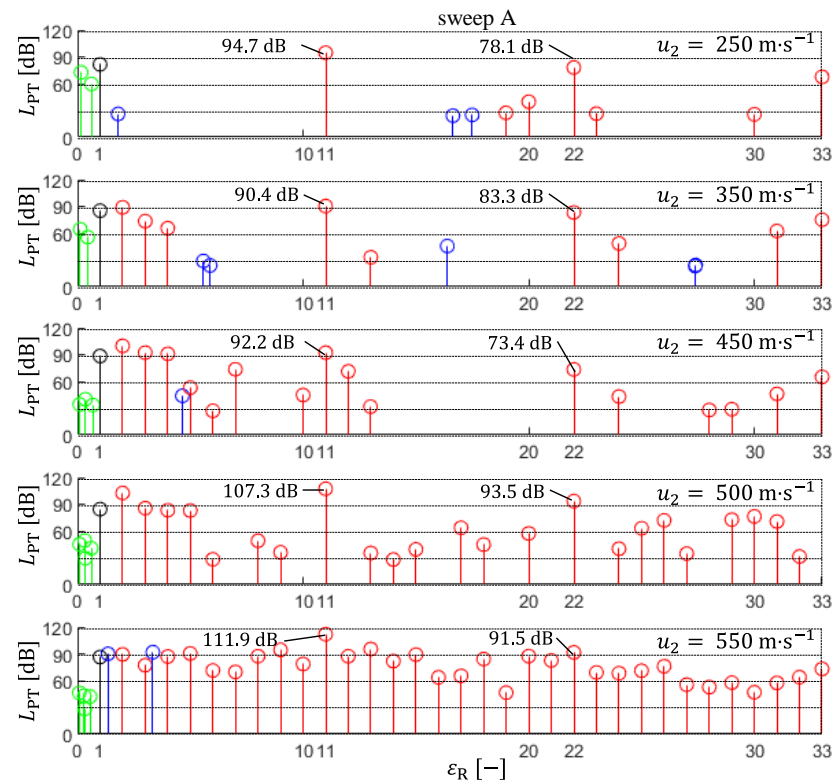


Figure 10. Sound pressure level of prominent tones for sweep A in the frequency spectrum as a function of ϵ_R . Green indicates sub-synchronous tones, black indicates synchronous tones, blue indicates super-synchronous tones and red indicates super-harmonic tones.

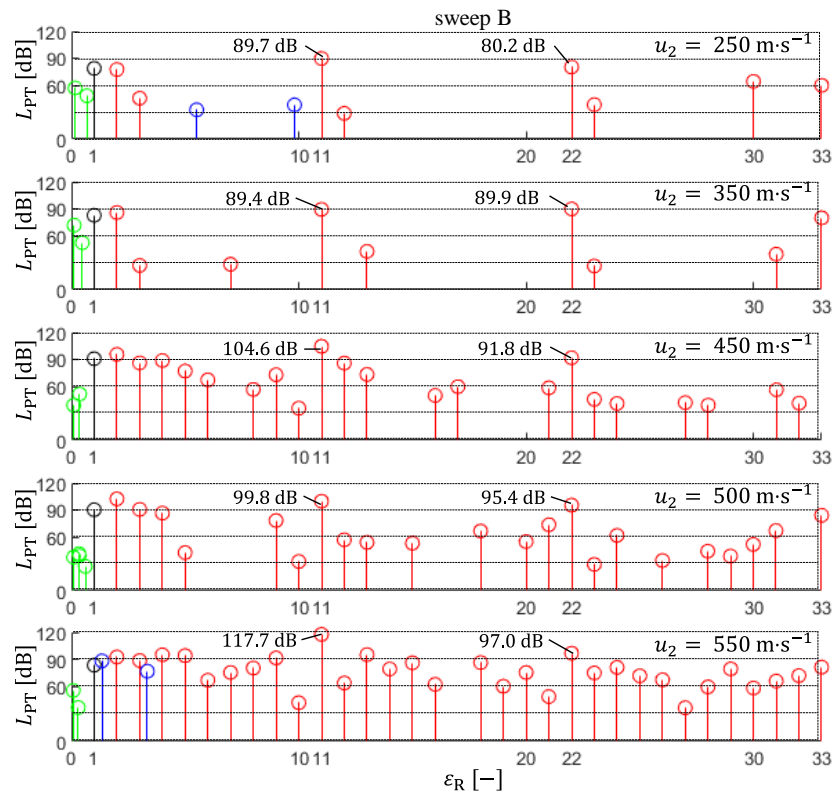


Figure 11. Sound pressure level of prominent tones for sweep B in the frequency spectrum as a function of ϵ_R . Green indicates sub-synchronous tones, black indicates synchronous tones, blue indicates super-synchronous tones and red indicates super-harmonic tones.

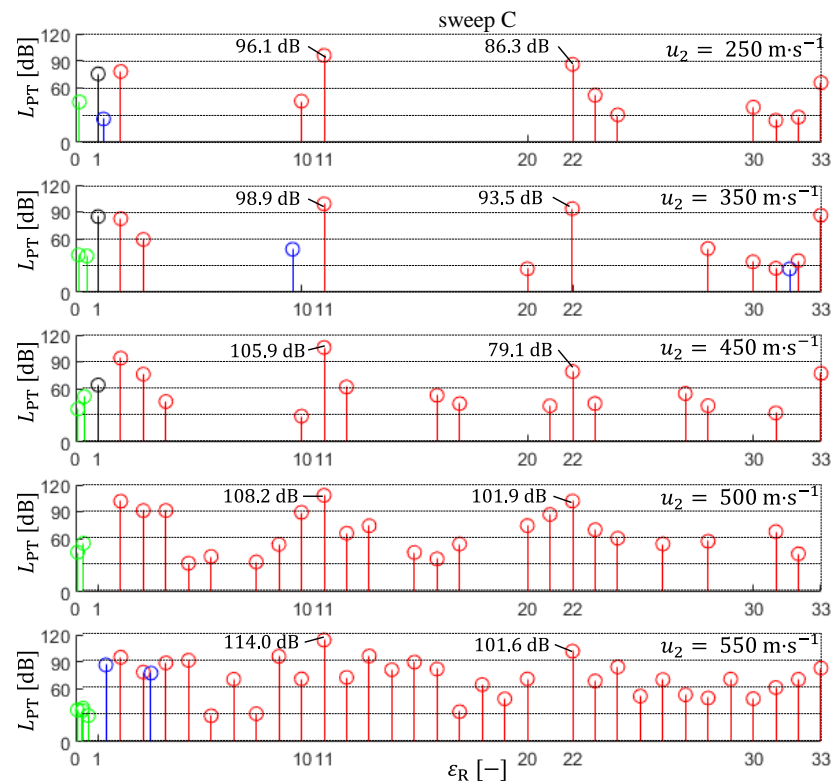


Figure 12. Sound pressure level of prominent tones for sweep C in the frequency spectrum as a function of ϵ_R . Green indicates sub-synchronous tones, black indicates synchronous tones, blue indicates super-synchronous tones and red indicates super-harmonic tones.

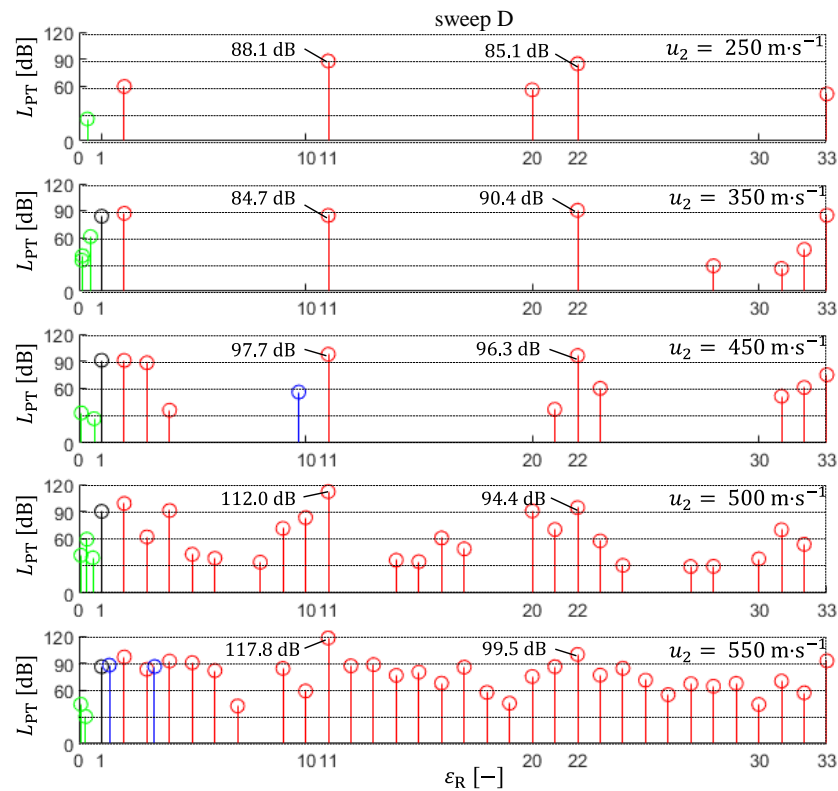


Figure 13. Sound pressure level of prominent tones for sweep D in the frequency spectrum as a function of ϵ_R . Green indicates sub-synchronous tones, black indicates synchronous tones, blue indicates super-synchronous tones and red indicates super-harmonic tones.

At all rotor speeds and at all sweeps, the tonal components of the blade-related noise can be identified. The metrics also show the presence of sub-synchronous frequency components that are very likely related to constant tone noise. This type of noise is due to instabilities in the inner lubrication layer of the hydrodynamic semi-floating ring bearings. In addition, the results show synchronous tones that are probably related to rotor unbalance and most likely to buzz-saw noise at higher speeds. At higher rotor speeds ($u_2 = 500 \text{ m}\cdot\text{s}^{-1}$ and $u_2 = 550 \text{ m}\cdot\text{s}^{-1}$), mainly super-harmonic components appear, which confirms the presence of buzz-saw noise at all four sweeps. The occurrence of super-synchronous tonal components in the frequency spectrum is relatively limited.

Furthermore, it can be noticed that the $L_P(A)_{\text{MBPF}}$ at sweep C shows an increasing trend as the rotor speed increases, whereas this trend cannot be confirmed at sweeps A, B and D. It is interesting to note that the lowest $L_P(A)_{\text{MSBPF}}$ at sweeps A and C is achieved at $u_2 = 450 \text{ m}\cdot\text{s}^{-1}$. Moreover, at all the measured points, the $L_P(A)$ is higher at the MBPF than at the MSBPF, with two exceptions: the operating points at sweeps B and D at $u_2 = 350 \text{ m}\cdot\text{s}^{-1}$. In addition, a significant difference between $L_P(A)_{\text{MBPF}}$ and $L_P(A)_{\text{MSBPF}}$ can be observed at sweeps A and C at $u_2 = 450 \text{ m}\cdot\text{s}^{-1}$, whereas at sweeps B and D, this difference is substantially lower.

The tonal metric allows the identification of tonal components in terms of frequency distribution. These tonal components can also be evaluated in terms of energy. The energy transmitted by a given tone or tones relative to the total compressor noise energy can be expressed in terms of the energy significance of the tone as

$$\psi_{\epsilon_{R,i}} = \frac{\sum_1^N p_{\epsilon_{R,i}}^2}{p_{\text{ef,tot}}^2}, \tag{11}$$

where $p_{\epsilon_{R,i}}$ is the effective pressure corresponding to the given tone. Equation (11) can be considered valid provided that the measurement is made under repeated conditions (density, speed of sound) in a free acoustic field, which was observed in the technical experiment.

An evaluation of the energy significance of the sum of tones 11, 22 and 33 shows that these tonal components are quite significant and at higher speeds comprise up to 70% of the total acoustic energy transmitted by the sound at the measurement location of the microphone (Figure 14). These tones are likely to correspond to noise primarily of the rotating blade-related noise type and are related to blade and compressor tongue interactions. It should be noted that tones 11, 22 and 33 also represent buzz-saw noise. However, given the insignificance of the other tonal components, that is, 1–10, 12–21 and 23–32 with respect to tone 11, this type of noise is unlikely to be significant. This means that the MBPF is the most significant component of buzz-saw noise.

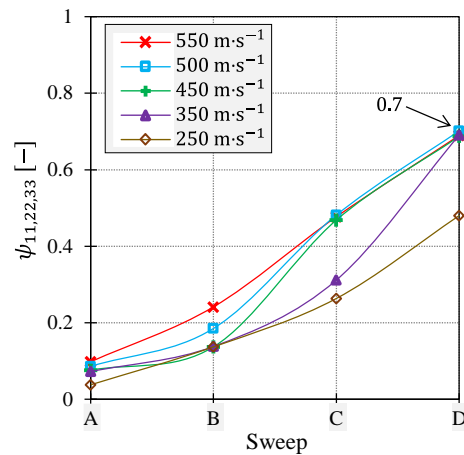


Figure 14. Energy significance of the sum of tones 11, 22 and 33 for sweeps A–D for analysed rotor speeds u_2 .

When evaluating the energy significance of the tones that are likely to correspond to a buzz-saw noise, it can be concluded that these components are only marginally significant for a given compressor because the energy significance does not exceed 7% (Figure 15).

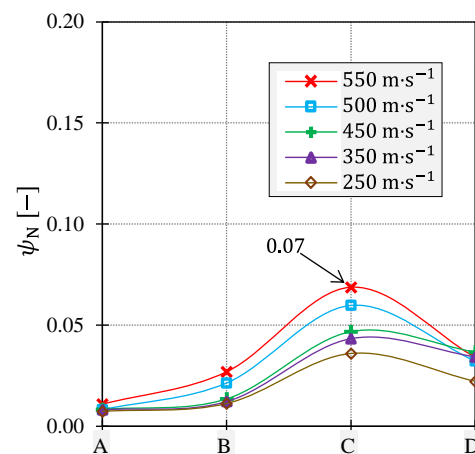


Figure 15. Energy significance of the sum of tones $N = 2 \dots 10; 12 \dots 21; 23 \dots 32$ for sweeps A–D for analysed rotor speeds u_2 .

Figures 14 and 15 present the energy significance of the selected tones. The remainder consists of the sub-synchronous components, the synchronous component and the super-synchronous components (sub-integer multiples) or broadband frequency components.

5. Conclusions

The measuring of the external acoustic field makes it possible to identify the dominant noise sources of aerodynamic origin and to quantify their influence at selected operating points. In the case of the centrifugal compressor presented here, the influence of integral multiples of the rotational frequency was dominant at all measured operating points and can therefore be considered the most significant contributor to the psychoacoustic impact on humans. The analysed acoustic spectrum also showed an increase in the number of tonal components with increasing rotor speed, which is due to shock waves—that is, buzz-saw noise—typical of the supersonic operating mode of a centrifugal compressor.

However, the detailed characteristics of aerodynamic phenomena, such as the number of stall cells and their rotational frequency in the case of rotating stall, cannot in principle be reliably determined this way. Measurements of the external acoustic field can therefore be used for a more global assessment of the influence of individual noise types. It is also worth mentioning that Kelvin–Helmholtz instability can occur precisely at the BPF [48], and the presence of tonality can therefore to some extent be influenced by it. However, its detection based on external acoustic field measurements is uncertain; one needs to find local maxima at the BPF in the time domain and form an envelope from them. If these maxima have the same value, that is, the amplitude of the BPF is constant in time, one could conclude that no other aerodynamic phenomenon is present at the BPF. However, in the opposite case, where the BPF amplitude changes over time, it is not clear from the acoustic measurements what effects are responsible for these changes. For the sampling frequency of 65,536 Hz used and the lowest measured rotor speed $u_2 = 250 \text{ m}\cdot\text{s}^{-1}$, the number of points describing the MBPF in the time domain was 17. In the case of the maximum measured rotor speed $u_2 = 550 \text{ m}\cdot\text{s}^{-1}$, there were only seven of these points. Thus, the number of measured points describing the MBPF in this case was insufficient to correctly predict the possible time history of the pressure fluctuations in the amplitude.

The acoustic spectrum presented here does not show broadband TCN. The absence of TCN, due to the occurrence of aerodynamic instabilities in the tip clearance region, may to some extent have been caused by the fact that the experimental compressor configuration consisted of an open loop with no inlet duct attached to the compressor impeller inlet. Therefore, it cannot be excluded that the rotor-rotating instabilities in this case were different from those in cases where an inlet duct is used.

Some of the implications of this research are quite serious, as it demonstrated the unpredictability of the sound pressure level for individual operating points, as discussed in Section 4. The analysis of the measured sound pressure levels did not show a clear trend in the aerodynamic noise at points on a given speed line and indicated an ambiguous relationship between the $L_P(A)_{\text{MBPF}}$ and the $L_P(A)_{\text{MSBPF}}$ at each operating point. This unpredictability probably stems from the complexity and non-linearity of the flow field itself. Therefore, the results presented here cannot be generalised and should be seen as somewhat limited to the rotating machine, although they do show a typical global trend of increasing total sound pressure levels at higher rotor speeds and surge. However, the elucidation of aerodynamic phenomena leading to a deeper understanding of the acoustic spectrum presented here requires additional measurement techniques. These include, for example, the use of high-frequency pressure probes to detect rotating stall characteristics.

Author Contributions: J.V. did signal processing and wrote the paper, P.N. developed tonal metrics and reviewed the paper. All authors have read and agreed to the published version of the manuscript.

Funding: The research that led to these results was funded by the FSI Science Fund project at Brno University of Technology, reg. no. FV22-19.

Institutional Review Board Statement: Not applicable.

Informed Consent Statement: Not applicable.

Data Availability Statement: Some or all data used in this research are available from the corresponding author by request.

Conflicts of Interest: The authors declare no conflict of interest.

References

1. Teymourpour, S.; Mahdavi-Vala, A.; Yadegari, M.; Kia, S.; Seydi, M.; Saboohi, Z. Engineering Approach for Noise Reduction for Automotive Radiator Cooling Fan: A Case Study. *SAE Tech. Pap.* **2020**, 1–12. [\[CrossRef\]](#)
2. Yadegari, M.; Ommi, F.; Saboohi, Z. Synergy between Noise Reduction Techniques Applied in Different Industries: A Review. *Int. J. Multiphys.* **2020**, *14*, 161–192.
3. Jansen, W. Rotating Stall in a Radial Vaneless Diffuser. *Trans. ASME J. Basic Eng.* **1964**, *86*, 750–758. [\[CrossRef\]](#)
4. Lennemann, E.; Howard, J. Unsteady Flow Phenomena in Rotating Centrifugal Impeller Passages. *J. Eng. Power* **1970**, *92*, 65–71. [\[CrossRef\]](#)
5. Senoo, Y.; Kinoshita, Y. Influence of Inlet Flow Conditions and Geometries of Centrifugal Vaneless Diffusers on Critical Flow Angle for Reverse Flow. *Trans. ASME J. Fluids Eng.* **1977**, *99*, 98–102. [\[CrossRef\]](#)
6. Senoo, Y.; Kinoshita, Y. Limits of Rotating Stall and Stall in Vaneless Diffuser of Centrifugal Compressors. In Proceedings of the ASME 1978 International Gas Turbine Conference and Products Show, London, UK, 9–13 April 1978; ASME Paper No. 78-GT-19. pp. 1–12.
7. Senoo, Y.; Ishida, M. Deterioration of Compressor Performance Due to Tip Clearance of Centrifugal Impellers. *J. Turbomach.* **1987**, *109*, 55–61. [\[CrossRef\]](#)
8. Greitzer, E. Surge and Rotating Stall in Axial Flow Compressors—Part I: Theoretical Compression System Model. *J. Eng. Power* **1976**, *98*, 190–198. [\[CrossRef\]](#)
9. Greitzer, E. Surge and Rotating Stall in Axial Flow Compressors—Part II: Experimental Results and Comparison with Theory. *J. Eng. Power* **1976**, *98*, 199–211. [\[CrossRef\]](#)
10. Kameier, F.; Neise, W. Rotating blade flow instability as a source of noise in axial turbomachines. *J. Sound Vib.* **1997**, *203*, 833–853. [\[CrossRef\]](#)
11. Osborn, W.; Lewis, G.; Heidelberg, L. *Effect of Several Porous Casing Treatments on Stall Limit and on Overall Performance of an Axial Flow Compressor Rotor*; NASA TN D-6537; NASA: Washington, DC, USA, 1971; pp. 1–50.
12. Fujita, H.; Takata, H. A Study on Configurations of Casing Treatment. *Bull. JSME* **1984**, *27*, 1675–1681. [\[CrossRef\]](#)
13. Bailey, E. *Effect of Grooved Casing Treatment on the Flow Range Capability of a Single-Stage Axial-Flow Compressor*; NASA TM X-2459; NASA: Washington, DC, USA, 1972; pp. 1–17.
14. Evans, D.; Ward, A. Minimising Turbocharger Whoosh Noise for Diesel Powertrains. In Proceedings of the SAE 2005 Noise and Vibration Conference and Exhibition 2005, Traverse City, MI, USA, 16–19 May 2005; pp. 1–10.
15. Schleer, M.; Song, S.; Abhari, R. Clearance Effects on the Onset of Instability in a Centrifugal Compressor. *J. Turbomach.* **2008**, *130*, 031002. [\[CrossRef\]](#)
16. Semlitsch, B.; Jyothishkumar, V.; Mihaescu, M.; Fuchs, L.; Gutmark, E. Investigation of the Surge Phenomena in a Centrifugal Compressor Using Large Eddy Simulation. In Proceedings of the ASME 2013 International Mechanical Engineering Congress and Exposition 2013, San Diego, CA, USA, 13–21 November 2013; pp. 1–10.
17. Sun, H.; Lee, S. Numerical prediction of centrifugal compressor noise. *J. Sound Vib.* **2004**, *269*, 421–430. [\[CrossRef\]](#)
18. Ohta, Y.; Takehara, N.; Okutsu, Y.; Outa, E. Effects of diffuser vane geometry on interaction noise generated from a centrifugal compressor. *J. Therm. Sci.* **2005**, *14*, 321–328. [\[CrossRef\]](#)
19. Ingenito, J.; Roger, M. Measurement and Prediction of the Tonal Noise of a Centrifugal Compressor at Inlet. In Proceedings of the 15th AIAA/CEAS Aeroacoustics Conference (30th AIAA Aeroacoustics Conference), Miami, FL, USA, 11–13 May 2009; pp. 1–18.
20. Liu, C.; Cao, Y.; Zhang, W.; Ming, P.; Liu, Y. Numerical and experimental investigations of centrifugal compressor BPF noise. *Appl. Acoust.* **2019**, *150*, 290–301. [\[CrossRef\]](#)
21. Marsan, A.; Moreau, S. Aeroacoustic Analysis of the Tonal Noise of a Large-Scale Radial Blower. *J. Fluids Eng.* **2018**, *140*, 021103. [\[CrossRef\]](#)
22. Zamiri, A.; Park, K.; Choi, M.; Chung, J. Transient Analysis of Flow Unsteadiness and Noise Characteristics in a Centrifugal Compressor with a Novel Vaned Diffuser. *Appl. Sci.* **2021**, *11*, 3191. [\[CrossRef\]](#)
23. Wang, P.; Zangeneh, M.; Heyes, F.; Roach, P. Multi-objective design of a transonic turbocharger compressor with reduced noise and increased efficiency. In Proceedings of the ASME Turbo Expo 2019: Turbomachinery Technical Conference and Exposition, Phoenix, AZ, USA, 17–21 June 2019; GT2019-90554. pp. 1–20.
24. Mao, Y.; Fan, C.; Zhang, Z.; Song, S.; Xu, C. Control of noise generated from centrifugal refrigeration compressor. *Mech. Syst. Signal Process.* **2021**, *152*, 107466. [\[CrossRef\]](#)
25. Torija, A.; Li, Z.; Chaitanya, P. Psychoacoustic modelling of rotor noise. *J. Acoust. Soc. Am.* **2022**, *151*, 1804–1815. [\[CrossRef\]](#)
26. Novaković, T.; Ogris, M.; Prezelj, J. Validating impeller geometry optimization for sound quality based on psychoacoustics metrics. *Appl. Acoust.* **2020**, *157*, 107013. [\[CrossRef\]](#)
27. Vacula, J.; Novotný, P. An Overview of Flow Instabilities Occurring in Centrifugal Compressors Operating at Low Flow Rates. *J. Eng. Gas Turbines Power* **2021**, *143*, 111002. [\[CrossRef\]](#)
28. Raitor, T.; Neise, W. Sound generation in centrifugal compressors. *J. Sound Vib.* **2008**, *314*, 738–756. [\[CrossRef\]](#)
29. Marshall, F.; Sorokes, J. A Review of Aerodynamically Induced Forces Acting on Centrifugal Compressors, and Resulting Vibration Characteristics Of Rotors. In Proceedings of the 29th Turbomachinery Symposium 2000, Houston, TX, USA, 18–21 September 2000; pp. 263–280.

30. Sundström, E.; Semlitsch, B.; Mihăescu, M. Centrifugal Compressor: The Sound of Surge. In Proceedings of the 21st AIAA/CEAS Aeroacoustics Conference 2015, Dallas, TX, USA, 22–26 June 2015; pp. 1–17.
31. Broatch, A.; Galindo, J.; Navarro, R.; García-Tiscar, J. Numerical and experimental analysis of automotive turbocharger compressor aeroacoustics at different operating conditions. *Int. J. Heat Fluid Flow* **2016**, *61*, 245–255. [[CrossRef](#)]
32. Qi, M.; Zhang, M.; Ma, C. Influences of Dis-Tuned Tip Clearance on the Discrete Aerodynamic Noise in Centrifugal Compressor. In Proceedings of the International Symposium on Transport Phenomena and Dynamics of Rotating Machinery 2016, Honolulu, HI, USA, 10–15 April 2016; pp. 1–7.
33. Chen, H. Noise of Turbocharger Compressors. In Proceedings of the 17th International Symposium on Transport Phenomena and Dynamics of Rotating Machinery ISROMAC2017, Maui, HI, USA, 16–21 December 2017; pp. 1–15.
34. Alqaradawi, M.; Shahin, I.; Gadala, M.; Badr, O. Aeroacoustic Simulation for NASA CC3 Centrifugal Compressor Operating at off Design Condition. *MATEC Web Conf.* **2016**, *70*, 030047. [[CrossRef](#)]
35. Zhang, Q.; Mao, Y.; Zhou, H.; Zhao, C.; Diao, Q.; Qi, D. Vibro-acoustics of a pipeline centrifugal compressor. *Appl. Acoust.* **2018**, *132*, 152–166. [[CrossRef](#)]
36. McAlpine, A.; Fisher, M. On the prediction of “buzz-saw” noise in aero-engine inlet ducts. *J. Sound Vib.* **2001**, *248*, 123–149. [[CrossRef](#)]
37. Morfey, C.; Fisher, M. Shock-wave radiation from a supersonic ducted rotor. *Aeronaut. J.* **1970**, *74*, 579–585. [[CrossRef](#)]
38. Tang, X.; Li, X. Prediction of “buzz-saw” noise propagation under nonuniform axial and radial flows. *AIP Adv.* **2020**, *10*, 055004. [[CrossRef](#)]
39. Sharma, S.; Broatch, A.; García-Tiscar, J.; Nickson, A.; Allport, J. Acoustic and pressure characteristics of a ported shroud turbocompressor operating at near surge conditions. *Appl. Acoust.* **2019**, *148*, 434–447. [[CrossRef](#)]
40. Thisse, J.; Polacsek, C.; Léwy, S.; Lafitte, A. On the generation and propagation of multiple pure tones inside turbofans at transonic regime. In Proceedings of the 20th AIAA/CEAS Aeroacoustics Conference 2014, Atlanta, GA, USA, 16–20 June 2014; pp. 1–14.
41. Toyama, K.; Runstadler, P.; Dean, R. An Experimental Study of Surge in Centrifugal Compressors. *J. Fluids Eng.* **1977**, *99*, 115–124. [[CrossRef](#)]
42. Oakes, W.; Lawless, P.; Fagan, J.; Fleeter, S. High speed centrifugal compressor surge initiation characterization. *J. Propuls. Power* **2002**, *18*, 1–11. [[CrossRef](#)]
43. Fink, D.; Cumpsty, N.; Greitzer, E. Surge Dynamics in a Free-Spool Centrifugal Compressor System. *J. Turbomach.* **1992**, *114*, 321–332. [[CrossRef](#)]
44. Ribi, B.; Gyarmathy, G. Impeller Rotating Stall as a Trigger for the Transition from Mild to Deep Surge in a Subsonic Centrifugal Compressor. In Proceedings of the ASME 1993 International Gas Turbine and Aeroengine Congress and Exposition, 3A, Cincinnati, OH, USA, 24–27 May 1993; pp. 1–12.
45. Hong, S.; Schleer, M.; Abhari, R. Effect of Tip Clearance on the Flow and Performance of a Centrifugal Compressor. In Proceedings of the ASME/JSME 2003 4th Joint Fluids Summer Engineering Conference 2003, Honolulu, HI, USA, 6–10 July 2003; pp. 1–7.
46. Andersen, J.; Lindström, F.; Westin, F. Surge Definitions for Radial Compressors in Automotive Turbochargers. *SAE Int. J. Engines* **2008**, *1*, 218–231. [[CrossRef](#)]
47. Kämmer, N.; Rautenberg, M. An Experimental Investigation of Rotating Stall Flow in a Centrifugal Compressor. In Proceedings of the ASME 1982 International Gas Turbine Conference and Exhibit, London, UK, 18–22 April 1982; Paper No: 82-GT-82 1982. Volume 1: Turbomachinery, pp. 1–9.
48. Bousquet, Y.; Binder, N.; Dufour, G.; Carbonneau, X.; Trebinjac, I.; Roumeas, M. Numerical Investigation of Kelvin–Helmholtz Instability in a Centrifugal Compressor Operating Near Stall. *J. Turbomach.* **2016**, *138*, 071007. [[CrossRef](#)]
49. Zheng, X.; Liu, A. Experimental Investigation of Surge and Stall in a High-Speed Centrifugal Compressor. *J. Propuls. Power* **2015**, *31*, 1–11.
50. Galindo, J.; Serrano, J.; Climent, H.; Tiseira, A. Experiments and modelling of surge in small centrifugal compressor for automotive engines. *Exp. Therm. Fluid Sci.* **2008**, *32*, 818–826. [[CrossRef](#)]
51. Dehner, R.; Selamet, A.; Keller, P.; Becker, M. Simulation of Deep Surge in a Turbocharger Compression System. *J. Turbomach.* **2016**, *138*, 111002. [[CrossRef](#)]
52. Teng, C.; Homco, S. Investigation of Compressor Whoosh Noise in Automotive Turbochargers. *SAE Int. J. Passeng. Cars Mech. Syst.* **2009**, *2*, 1345–1351. [[CrossRef](#)]
53. Navarro, R. A Numerical Approach for Predicting Flow-Induced Acoustics at Near-Stall Conditions in an AUTOMOTIVE turbocharger Compressor. Ph.D. Thesis, Universitat Politècnica de València, Valencia, Spain, 2014.
54. Japikse, D. *Centrifugal Compressor Design and Performance*; Concepts ETI, Inc.: Norwich, VT, USA, 1996; ISBN 0-933283-03-2.
55. Bousquet, Y.; Carbonneau, X.; Dufour, G.; Binder, N.; Trebinjac, I. Analysis of the Unsteady Flow Field in a Centrifugal Compressor from Peak Efficiency to Near Stall with Full-Annulus Simulations. *Int. J. Rotating Mach.* **2014**, *2014*, 729629. [[CrossRef](#)]
56. Mendonça, F.; Baris, O.; Capon, G. Simulation of Radial Compressor Aeroacoustics Using CFD. *Proc. ASME Turbo Expo.* **2012**, *8*, 1823–1832.
57. Fontanesi, S.; Paltrinieri, S.; Cantore, G. CFD analysis of the acoustic behavior of a centrifugal compressor for high performance engine application. *Energy Procedia* **2014**, *45*, 759–768. [[CrossRef](#)]
58. Jyothishkumar, V.; Mihaescu, M.; Semlitsch, B.; Fuchs, L. Numerical Flow Analysis in a Centrifugal Compressor near Surge Condition. In Proceedings of the 43rd Fluid Dynamics and Co-located Conferences, San Diego, CA, USA, 24–27 June 2013; pp. 1–13.

59. Sundström, E.; Semlitsch, B.; Mihaescu, M. Acoustic signature of flow instabilities in radial compressors. *J. Sound Vib.* **2018**, *434*, 221–236. [[CrossRef](#)]
60. Semlitsch, B.; Mihăescu, M. Flow phenomena leading to surge in a centrifugal compressor. *Energy* **2016**, *103*, 572–587. [[CrossRef](#)]
61. Fastl, H.; Zwicker, E. *Psychoacoustics: Facts and Models*, 3rd ed.; Springer: Berlin/Heidelberg, Germany, 2007; ISBN 35-402-3159-5.

Disclaimer/Publisher’s Note: The statements, opinions and data contained in all publications are solely those of the individual author(s) and contributor(s) and not of MDPI and/or the editor(s). MDPI and/or the editor(s) disclaim responsibility for any injury to people or property resulting from any ideas, methods, instructions or products referred to in the content.